Nanoscale

COMMUNICATION

View Article Online
View Journal

Cite this: DOI: 10.1039/d5nr03069b

Received 21st July 2025,
Accepted 28th October 2025

DOI: 10.1039/d5nr03069b

rsc.li/nanoscale

Enhanced CO_2 affinity in a metal–organic framework through green incorporation of a dual-functional amino acid

Edward Loukopoulos, *[a,c] Sofía Barragán-Soto,[a] Sergio Marugán-Benito,[a] Emilio Borrego-Marin, [b] Jorge A. R. Navarro [b] and Ana E. Platero-Prats *†[a,c]

Post-synthetic incorporation of amino acids into the Zr-based metal–organic framework DUT-67 *via* relatively green methods yields materials with enhanced CO_2 affinity. Structural and sorption studies reveal high affinity for DUT-67-Trp, exploiting its dual functionality to achieve an adsorption enthalpy level comparable to those of high-performing frameworks. The findings provide a promising pathway towards developing sustainable amino-functionalized CO_2 sorbents.

The increasing environmental concerns about climate change and air pollution have resulted in a constant search for innovative solutions that can reduce greenhouse gas emissions, with carbon dioxide being a top priority.[1] Currently, the most common CO_2 removal processes utilize amine-based materials, including liquid solutions[2,3] as well as porous solids like zeolites,[4] silica,[5] and covalent-[6,7] or metal–organic frameworks (MOFs).[8,9] The success of this approach relies on the favourable interactions between CO_2 and the sorbent through formation of carbamate/bicarbonate intermediates.[10] A particularly promising method involves incorporation of alkylamines into MOFs,[11–14] producing solid adsorbents with the potential to capture CO_2 directly from air.[15] This strategy has led to considerable advancements of the field, yet improved amine-based methods still need to be optimized to overcome existing operational limitations in capture performance (capacity and selectivity), recyclability (high regeneration energies) and material stability (amine loss over multiple cycles).[16,17] Another crucial, often overlooked factor in these processes is their detrimental effect on the environment potentially caused by their regular use of hazardous amino species like alkylamines. Integrating sustainable chemicals and practices is essential at all stages of functional material development,[18] particularly in materials intended for environmental applications.

In this context, developing MOF sorbents incorporating amino acids offers a sustainable and efficient approach for material design. Amino acids are inexpensive and abundant chemicals that do not pose the hazards of alkylamines. By coupling the various options in length and basicity of amino acids with the high surface areas, stability and tuneable chemistry of MOFs, the pores and surfaces of the resulting functionalized materials can be precisely tuned and hence provide an excellent opportunity to improve CO_2 affinity.[11,16] Furthermore, the carboxylate group in amino acids enables the amino acids to be directly bound to MOFs through M–O coordination bonding, orienting the amino group towards the pores. This arrangement offers new options compared to alkylamine-modified frameworks, as it provides access to inorganic nodes displaying higher stability, reducing the amine loss during CO_2 capture cycles.

Building on this approach, we report the post-synthetic incorporation of two different amino acids, namely L-proline (Pro) or L-tryptophan (Trp), into the much-studied Zr-based MOF DUT-67. The pristine framework is based on 8-connected Zr_6O_8 nodes (Fig. 1A), utilizing 2,5-thiophenedicarboxylate (TDC) as the organic ligand.[19] Its well-known inorganic cluster combines high stability with tuneable composition, containing unsaturated Zr centres for amino-acid functionalization (Fig. 1B). The resulting frameworks, DUT-67-Pro and DUT-67-Trp, are prepared in ethanol and display improved CO_2 affinity compared to the initial DUT-67, as determined from adsorption studies. Notably, DUT-67-Trp exhibits an isosteric enthalpy of CO_2 adsorption of 50 kJ mol^{-1}, a marked improvement over the value observed for the pristine framework (31.8 kJ mol^{-1}), and comparable to those of high-performance amine-modified MOFs without hazardous reagents and with no chemical degradation after capture. Short- and long-range structural studies indicate an increased CO_2 selectivity through

[a]*Departamento de Química Inorgánica, Facultad de Ciencias, Universidad Autónoma de Madrid, Campus de Cantoblanco, 28049 Madrid, Spain. E-mail: edouardos.loukopoulos@uam.es, ana.platero@uam.es*

[b]*Departamento de Química inorgánica, Universidad de Granada, 18071 Granada, Spain*

[c]*Condensed Matter Physics Center (IFIMAC), Universidad Autónoma de Madrid, Campus de Cantoblanco, 28049 Madrid, Spain*

†Present address: Institute of Catalysis and Petrochemistry (ICP-CSIC), Universidad Autónoma de Madrid, Campus de Cantoblanco, 28049 Madrid, Spain.

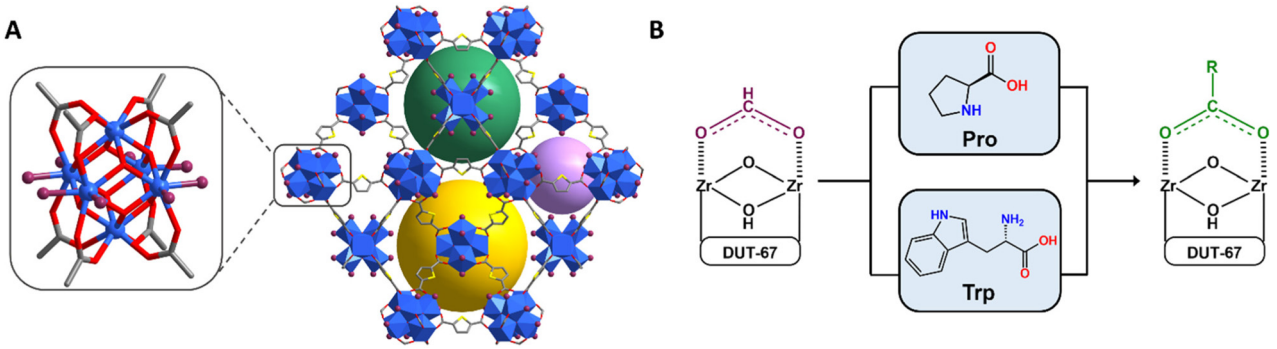

Fig. 1 (A) View of the 8-connected Zr_6 cluster in DUT-67 (left) and the framework of DUT-67, highlighting the different types of pores (right). Color coding: Zr = blue, C = grey, O = red. Dark purple spheres in the Zr_6O_8 nodes indicate the potentially available functionalization positions. H atoms have been omitted for clarity. (B) Schematic of the amino-acid functionalization of the inorganic node in DUT-67 as demonstrated in this work.

multiple potential interaction sites, uniquely facilitated by the presence of Trp. The results represent an important step towards the design of sustainable amine-based sorbents with enhanced potential for CO_2 capture.

Pristine DUT-67 was synthesized in high yields following a previously reported procedure (SI, Section S1).[20] As corroborated by powder X-ray diffraction (PXRD) and scanning electron microscopy (SEM) data (Fig. 2A, S1 and S2), the resulting solid displayed high crystallinity and phase purity. In particular, the corresponding PXRD pattern closely matched the simulated one from the crystal structure of DUT-67, while SEM images showed crystallites with dimensions in the range of 0.5–1 μm, in line with previous reports.[21] Further confirming the identity of this material, ^{1}H nuclear magnetic resonance (NMR) spectroscopy and thermogravimetric analysis (TGA) revealed the incorporation of 2 formate modulator molecules per Zr_6O_8 node (Fig. S3 and S4). These results translate to a chemical formula of $[Zr_6O_6(OH)_2(TDC)_4(HCOO)_2(solvent)_4]$ for the main framework, also in accordance with previous studies using this modulator.[21,22]

In the next step of our investigation, we aimed to functionalize DUT-67 with either Pro or Trp by performing a post-syn-

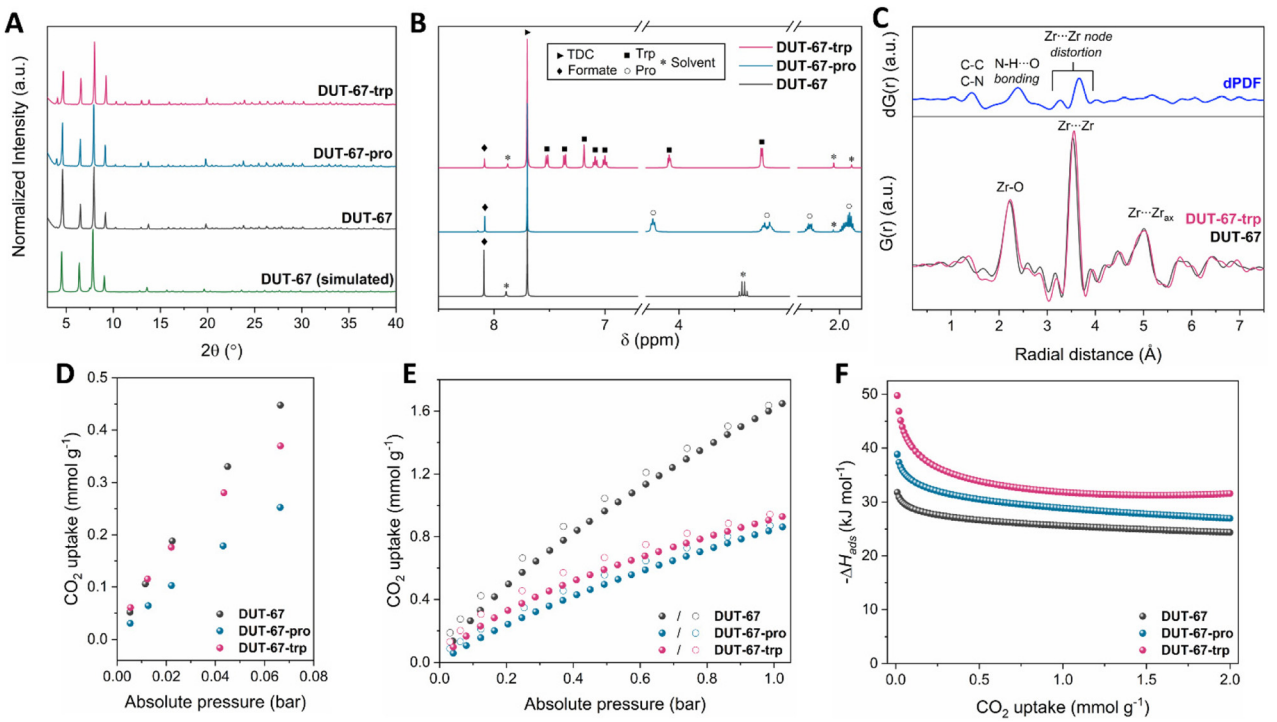

Fig. 2 (A) PXRD data for all MOFs of this study. (B) Selected peaks of the ^{1}H-NMR spectra for all materials after digestion, indicating presence of amino acids in the functionalized analogues. The full spectra can be found in the SI (Fig. S5 and S6). (C) PDF data of DUT-67 and DUT-67-Trp (bottom) and the corresponding dPDF signal (top), confirming tryptophan incorporation. (D) Low-pressure region of the CO_2 isotherms for all MOFs recorded at 273 K (full region shown in Fig. S13). (E) CO_2 isotherms for all MOFs recorded at 298 K. (F) Plots of the corresponding isosteric enthalpies of adsorption, calculated using the Clausius–Clapeyron equation from the 273 and 298 K adsorption data.

thetic amino-acid insertion within the unsaturated positions of the Zr_6O_8 nodes (Fig. 1B). This functionalization was performed by carrying out solvothermal incorporation experiments, in which the pristine solid was immersed in a solution of the targeted amino acid under predetermined conditions (SI, Section S2). To optimize the amount of amino acid loaded, a thorough screening of various synthetic parameters was carried out, including of different temperatures, solvents, reaction times and pH levels, as summarized in Table S1. The efficacy of each test was initially assessed by taking ^{1}H-NMR measurements of the resulting solids, allowing us to quantify the amount of amino acid incorporated (Fig. 2B, S5 and S6). Notably, the highest degree of functionalization for both ligands was afforded by performing reactions in ethanol, a green solvent,[23] thus avoiding the need for hazardous solvents such as dimethylformamide that is typically used to modify DUT-67.[20,22,24] As outlined in Section S2, complete cluster saturation was achieved in DUT-67-Pro, with four Pro molecules inserted per Zr_6O_8 node. In contrast, the greater bulkiness and higher $pK_{a_{COO-}}$ of Trp resulted in partial replacement of formates, leading to the incorporation of two Trp molecules per inorganic cluster.

Additional characterization was performed to conclusively determine the identities of the functionalized solids. In both materials, crystallinity and structural integrity of the main framework were maintained during the modification process according to the PXRD data (Fig. 2A, S7 and S8). As anticipated, N_2 adsorption studies at 77 K indicated that the introduction of bulkier ligands reduced the porosity of these MOFs, evidenced by decreased values in uptake, specific surface area, pore size and volume (Fig. S9, S10 and Table S2). Complementary Fourier-transform infrared spectroscopy (FT-IR) studies, detailed in Fig. S11, also revealed characteristic signals associated with the presence of the Zr_6O_8 cluster and amino groups, among others. Both spectra confirmed the absence of uncoordinated –COOH groups, indicating that the amino acids coordinated to the inorganic nodes rather than occupying the pores of the framework.

To further investigate the local structural features within these MOFs, pair distribution function (PDF) analysis was applied to total X-ray scattering data collected for representative materials DUT-67 and DUT-67-Trp. As seen in Fig. 2C and S12, in both cases the PDF showed three main peaks, at approximately 2.2, 3.5 and 5.0 Å, corresponding to Zr–O, Zr···Zr and Zr···Zr_{axial} pair correlations within the Zr_6O_8 clusters.[25] The impact of the post-synthetic modification was also evaluated by performing differential PDF (dPDF) analysis comparing the signals of the two materials. Key features were identified at 1.4 Å (C–C/C–N distances), 2.4 Å (intramolecular N–H···O bonding in Trp[26]), 3.3 and 3.7 Å (local distortion of the Zr_6O_8 nodes upon Trp replacing the initial non-structural ligands[27,28]), confirming amino-acid incorporation within the inorganic clusters.

Having assessed structural composition, CO_2 adsorption measurements were taken for all materials at 273 and 298 K. These measurements allowed us to evaluate the CO_2-capture abilities of these MOFs and to characterize the physicochemical nature of each adsorption process. All materials were activated *in vacuo* at 100 °C for 15 hours. Experiments with a batch of pristine DUT-67 at 273 and 298 K revealed respective uptakes of 2.99 and 1.60 mmol g^{-1} at a pressure of 1 bar (Fig. 2E and S13). These values were also found to be in very good agreement with those of other literature studies for this material.[29] Unsurprisingly, the incorporation of larger amino acids resulted in a significant decrease in uptake for both functionalized materials due to reduced available pore space. Specifically, uptakes of 1.66 (273 K) and 0.84 (298 K) mmol g^{-1} were observed for DUT-67-Pro at 1 bar, while the corresponding values for DUT-67-Trp were measured to be 1.73 (273 K) and 0.92 (298 K) mmol g^{-1} under the same conditions. A more thorough analysis of the isotherm data led to additional observations and conclusions. The adsorption branch for all frameworks showed steeper slopes at low pressure levels (up to 0.2 bar), with the steepness decreasing to various degrees for each MOF as the pressure was increased. These features indicated a distinct response for each material as CO_2 was introduced, pointing to differences between the gas-framework interactions of the different frameworks. Notably, at 273 K the Trp-functionalized material showed a higher uptake and steeper slope at low pressures, namely in the 0–2.5 kPa range, than displayed by the Pro-functionalized material, despite Trp being the bulkiest amino acid, suggesting a strong CO_2 preference. Furthermore, the desorption branch for all materials revealed practically reversible sorption processes, although slight hysteresis was observed, particularly at 298 K and more pronounced for DUT-67-Trp, indicating greater CO_2 affinity due to chemisorption.[30]

To corroborate these observations, the isosteric enthalpy of adsorption (ΔH_{ads}) was calculated for each of the materials from the Clausius–Clapeyron equation using the above data. For pristine DUT-67, a moderate $-\Delta H_{ads}$ of 31.8 kJ mol^{-1} was calculated at zero surface coverage. Both modified frameworks showed better adsorption enthalpies, as per the initial hypothesis—with the respective $-\Delta H_{ads}$ for the proline analogue increased to 38.8 kJ mol^{-1}, and that for the tryptophan-functionalized material considerably increased to 50 kJ mol^{-1}. This result provided evidence for the strong preference of DUT-67-Trp for CO_2, comparable to other high-performing MOFs in the field of CO_2 capture, including amino-functionality–containing materials (Table 1). Importantly, the strength of these gas-framework interactions is not excessively high, hence helping to minimize the energy required to desorb CO_2, and facilitating regeneration of the material. Furthermore, the strong affinity in DUT-67-Trp was achieved without the use of hazardous amines, as environmentally-friendly protocols were employed for both the synthesis of the pristine material and the post-synthetic modifications. PXRD and ^{1}H-NMR measurements following CO_2 sorption and vacuum treatment (Fig. S14 and S16) also showed that both functionalized materials retained their composition and crystallinity, indicating potential reusability over multiple cycles.

To evaluate the CO_2-capture performance of the materials under relatively ambient conditions, dynamic breakthrough

Table 1 Synthetic aspects and CO_2 affinity characteristics in representative high-performing metal–organic frameworks, including DUT-67-Trp

MOF material	$-\Delta H_{ads}$ (kJ mol^{-1})	Features	Ref.
HKUST-1	35	Open metal sites	31
Mg-MOF-74	47	Open metal sites	32
SIFSIX-3-Cu	54	Physisorption due to ultramicroporosity Use of hazardous azine	33
CAU-1	48	Amino-containing linker	34
NH_2-MIL-101(Cr)	~50	Open metal sites, amino-containing linker	35
Cu-BTTri-en	90	Open metal sites, amino functionalization Use of hazardous diamine	30
Hydrazine-Mg-MOF-74	90	Open metal sites, amino functionalization Use of hazardous diamine	36
en-MIL-100(Cr) mmen-MIL-100(Cr)	80	Open metal sites, amino functionalization Use of hazardous amine	37
MOF-808-Gly	46	Open metal sites, amino functionalization Non-hazardous amine, green synthesis	16
MOF-808-DL-Lys	80	Open metal sites, amino functionalization Non-hazardous amine, DMSO synthesis	16
DUT-67-Trp	50	Open metal sites, amino functionalization Non-hazardous amine, green synthesis	This work

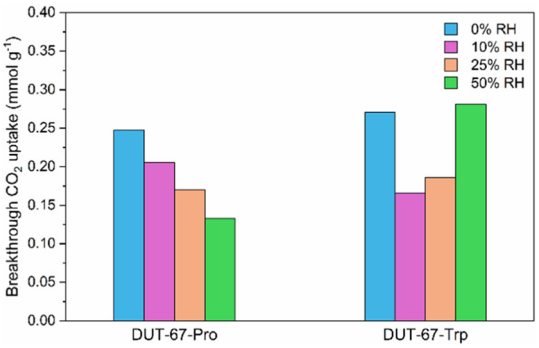

Fig. 3 CO_2 uptake values obtained from dynamic breakthrough experiments for DUT-67-Pro and DUT-67-Trp under various relative humidity (RH) conditions (0%, 10%, 25%, and 50%).

experiments were conducted (Fig. 3 and Section S5) for DUT-67-Pro and DUT-67-Trp. Samples of a simulated flue gas mixture of 15% CO_2 and 85% N_2 (20 mL min^{-1} total flow) with different levels of relative humidity (RH), ranging from 0 to 50%, were tested to assess the effect of water vapor on the adsorption process. The results revealed a clear difference between the breakthrough profiles for DUT-67-Pro and DUT-67-Trp. Initially, both materials exhibited a decrease in uptake with increasing humidity (10% RH). This initial decline may be attributed to competitive adsorption of water, likely *via* hydrogen-bonding interactions with the amino-acid functional groups. Interestingly, at higher relative humidity (25–50%) the tryptophan-functionalised analogue tended to recover its initial adsorption efficiently, eventually approaching the behaviour observed under dry conditions. This result suggested that once a hydration equilibrium was reached, further water uptake no longer compromised the accessibility of CO_2 adsorption sites in the case of DUT-67-Trp. These findings underscored the effects of amino-acid selection and moisture on the adsorption mechanism, revealing a humidity-tolerant behaviour at elevated RH.

In order to assess the cyclability of the materials, we then tested the DUT-67-Pro and DUT-67-Trp systems over three consecutive breakthrough cycles at 50% RH (Fig. S23). The results indicated a slight drop in adsorption capacity (10% for the Trp derivative and 19% for the Pro system) from cycle 1 to cycle 2, followed by subsequent maintenance of adsorption capacity. The larger drop in adsorption capacity for DUT-67-Pro was consistent with its higher sensitivity to moisture. The collective data from CO_2 affinity, breakthrough and recyclability experiments confirmed the superior stability and performance of the Trp-functionalized material in comparison to the Pro-analogue.

Upon considering the chemical composition of our materials, it became evident that multiple factors could be used to optimize CO_2 binding. The presence of amino groups and unsaturated Zr_6O_8 nodes were indicated to be key driving forces: up to four active metal sites per cluster can be made available in pristine DUT-67 after removal of coordinating solvent molecules. With all these positions occupied by $-COO_{proline}$ groups in DUT-67-Pro, CO_2 affinity was further enhanced by the incorporated amino groups, as the CO_2 molecules and amino groups reacted under dry conditions to form the well-reported carbamate intermediate (Fig. S17).[10,12,16] DUT-67-Trp combined both elements, with each Zr_6O_8 node featuring two amino acid molecules and at least one open metal site after activation, consistent with its superior performance. Moreover, note formation of dipole-π interactions between the adsorbate and the indole ring of the amino acid appearing to be an important factor for boosting CO_2 adsorption preference in the Trp analogue.[38] This formation could explain the marked differences in affinity between the two functionalized MOFs, with DUT-67-Trp outperforming DUT-67-Pro despite having fewer amino groups, lower basicity ($pK_{a_{Trp}}$ = 9.39 and $pK_{a_{Pro}}$ = 10.36) and a bulkier amino acid. While theoretical calculations are currently underway to validate these observations, the results already highlighted tryptophan as a promising option for the greener design of amino-

acid–modified MOF systems with improved CO_2 adsorption potential. For all materials, the adsorption enthalpy values slightly decreased with increasing gas loading, indicating that after initial binding to these preferred locations, CO_2 was subsequently adsorbed onto less reactive sites.

Conclusions

In this study, we successfully demonstrated the post-synthetic incorporation of amino acids into the Zr_6O_8-based DUT-67 framework, resulting in materials with enhanced CO_2 affinity. This methodology underscored a sustainable approach to material design and modification by introducing amino-containing molecules of minimal environmental impact *via* cleaner methods, addressing relevant concerns associated with typically used amines. Our findings indicated both amino groups and unsaturated Zr centres playing crucial roles in CO_2 binding, leading to increased affinity. Notably, DUT-67-Trp exhibited superior performance, attributed to the formation of dipole-π interactions and the availability of multiple active sites. This material achieved an isosteric enthalpy of adsorption of 50 kJ mol^{-1}, demonstrating a performance comparable to those of other leading CO_2 sorbents while eliminating the need for hazardous molecules. Furthermore, DUT-67-Trp retained a similar adsorption behaviour at high relative humidity levels. On the other hand, the large size of the used amino acids caused a trade-off in performance, leading to reduced CO_2 uptakes in comparison to the pristine MOF. Although this aspect limits the potential of DUT-67 as a suitable platform for practical use, this study has overall increased our understanding of the development of amino-acid–modified MOFs as promising CO_2 sorbent candidates, highlighting several beneficial directions. Future work is expected to aim to improve and expand this approach by utilizing other Zr_6O_8-based frameworks with larger pores to maximize CO_2 capacity. Additionally, investigation of a broader range of amino acids is planned to fully elucidate their chemical effects on adsorption enthalpy.

Author contributions

Conceptualization: E. L. and A. E. P. P. Methodology: E. L., J. A. R. N. and A. E. P. P. Formal analysis: E. L., S. B. S., S. M. B and E. B. M. Data curation: E. L., S. B. S., S. M. B and E. B. M. Project administration: E. L. and A. E. P. P. Funding acquisition: E. L. and A. E. P. P. Writing – original draft: E. L., S. B. S. and A. E. P. P. Writing – review and editing: all co-authors.

Conflicts of interest

There are no conflicts to declare.

Data availability

The data supporting this article have been included as part of the supplementary information (SI). Supplementary information is available. See DOI: https://doi.org/10.1039/d5nr03069b.

Acknowledgements

This project has received funding from the European Union's Horizon 2020 research and innovation programme under grant agreement No. 101034324. This work was supported by the grants PID2021-123839OB-I00, PID2023-147972OB-I00, RYC2018-024328-I and CNS2022-135261 funded by MICIU/AEI/10.13039/501100011033 and the NextGenerationEU/PRTR. The authors acknowledge the financial support from the Spanish Ministry of Science and Innovation, through the "María de Maeztu" Programme for Units of Excellence in R&D (CEX2018-000805-M and CEX2023-001316-M). The authors acknowledge the European Synchrotron Radiation Facility (ESRF) for provision of synchrotron radiation facilities (PDF experiments, proposal MA-5852), and the authors would like to thank Dr Stefano Checcia for assistance and support in using beamline ID15A.

References

1 *Climate Change 2022 – Mitigation of Climate Change: Working Group III Contribution to the Sixth Assessment Report of the Intergovernmental Panel on Climate Change*, ed. Intergovernmental Panel on Climate Change, Cambridge University Press, Cambridge, 2023, pp. 51–148, DOI: 10.1017/9781009157926.002.
2 M. E. Boot-Handford, J. C. Abanades, E. J. Anthony, M. J. Blunt, S. Brandani, N. Mac Dowell, J. R. Fernández, M. C. Ferrari, R. Gross, J. P. Hallett, R. S. Haszeldine, P. Heptonstall, A. Lyngfelt, Z. Makuch, E. Mangano, R. T. J. Porter, M. Pourkashanian, G. T. Rochelle, N. Shah, J. G. Yao and P. S. Fennell, *Energy Environ. Sci.*, 2014, **7**, 130–189.
3 G. T. Rochelle, *Science*, 2009, **325**, 1652–1654.
4 D. G. Boer, J. Langerak and P. P. Pescarmona, *ACS Appl. Energy Mater.*, 2023, **6**, 2634–2656.
5 G. Zhao, B. Aziz and N. Hedin, *Appl. Energy*, 2010, **87**, 2907–2913.
6 H. Li, A. Dilipkumar, S. Abubakar and D. Zhao, *Chem. Soc. Rev.*, 2023, **52**, 6294–6329.
7 H. Lyu, H. Li, N. Hanikel, K. Wang and O. M. Yaghi, *J. Am. Chem. Soc.*, 2022, **144**, 12989–12995.
8 S. Mahajan and M. Lahtinen, *J. Environ. Chem. Eng.*, 2022, **10**, 108930.
9 K. Sumida, D. L. Rogow, J. A. Mason, T. M. McDonald, E. D. Bloch, Z. R. Herm, T. H. Bae and J. R. Long, *Chem. Rev.*, 2012, **112**, 724–781.

10 R. B. Said, J. M. Kolle, K. Essalah, B. Tangour and A. Sayari, *ACS Omega*, 2020, **5**, 26125–26133.
11 O. I. Chen, C. H. Liu, K. Wang, E. Borrego-Marin, H. Li, A. H. Alawadhi, J. A. R. Navarro and O. M. Yaghi, *J. Am. Chem. Soc.*, 2024, **146**, 2835–2844.
12 E. J. Kim, R. L. Siegelman, H. Z. H. Jiang, A. C. Forse, J. H. Lee, J. D. Martell, P. J. Milner, J. M. Falkowski, J. B. Neaton, J. A. Reimer, S. C. Weston and J. R. Long, *Science*, 2020, **369**, 392–396.
13 T. M. McDonald, J. A. Mason, X. Kong, E. D. Bloch, D. Gygi, A. Dani, V. Crocellà, F. Giordanino, S. O. Odoh, W. S. Drisdell, B. Vlaisavljevich, A. L. Dzubak, R. Poloni, S. K. Schnell, N. Planas, K. Lee, T. Pascal, L. F. Wan, D. Prendergast, J. B. Neaton, B. Smit, J. B. Kortright, L. Gagliardi, S. Bordiga, J. A. Reimer and J. R. Long, *Nature*, 2015, **519**, 303–308.
14 A. Rubio-Gaspar, A. Misturini, R. Millan, N. Almora-Barrios, S. Tatay, V. Bon, M. Bonneau, V. Guillerm, M. Eddaoudi, S. Navalón, S. Kaskel, D. Armentano and C. Martí-Gastaldo, *Angew. Chem., Int. Ed.*, 2024, **63**, e202402973.
15 S. Bose, D. Sengupta, T. M. Rayder, X. Wang, K. O. Kirlikovali, A. K. Sekizkardes, T. Islamoglu and O. K. Farha, *Adv. Funct. Mater.*, 2023, **34**, 2307478.
16 H. Lyu, O. I. F. Chen, N. Hanikel, M. I. Hossain, R. W. Flaig, X. Pei, A. Amin, M. D. Doherty, R. K. Impastato, T. G. Glover, D. R. Moore and O. M. Yaghi, *J. Am. Chem. Soc.*, 2022, **144**, 2387–2396.
17 A. B. Rao and E. S. Rubin, *Environ. Sci. Technol.*, 2002, **36**, 4467–4475.
18 P. Marino, P. R. Donnarumma, H. A. Bicalho, V. Quezada-Novoa, H. M. Titi and A. J. Howarth, *ACS Sustainable Chem. Eng.*, 2021, **9**, 16356–16362.
19 V. Bon, I. Senkovska, J. D. Evans, M. Wöllner, M. Hölzel and S. Kaskel, *J. Mater. Chem. A*, 2019, **7**, 12681–12690.
20 E. Loukopoulos, S. Marugán-Benito, D. Raptis, E. Tylianakis, G. E. Froudakis, A. Mavrandonakis and A. E. Platero-Prats, *Adv. Funct. Mater.*, 2024, **34**, 2409932.
21 V. Bon, I. Senkovska, I. A. Baburin and S. Kaskel, *Cryst. Growth Des.*, 2013, **13**, 1231–1237.
22 F. Drache, V. Bon, I. Senkovska, C. Marschelke, A. Synytska and S. Kaskel, *Inorg. Chem.*, 2016, **55**, 7206–7213.
23 C. Capello, U. Fischer and K. Hungerbühler, *Green Chem.*, 2007, **9**, 927–993.
24 K. D. Nguyen, C. Kutzscher, F. Drache, I. Senkovska and S. Kaskel, *Inorg. Chem.*, 2018, **57**, 1483–1489.
25 I. Romero-Muñiz, E. Loukopoulos, Y. Xiong, F. Zamora and A. E. Platero-Prats, *Chem. Soc. Rev.*, 2024, **53**, 11772–11803.
26 R. A. Yadav, M. Yogesha, B. Yadav and C. Santhosh, *J. Mol. Struct.*, 2018, **1171**, 867–879.
27 J. M. Moreno, R. Gil-San-Millan, R. Mas-Ballesté, J. Alemán and A. E. Platero-Prats, *ChemCatChem*, 2024, **16**, e202400676.
28 A. E. Platero-Prats, A. Mavrandonakis, L. C. Gallington, Y. Liu, J. T. Hupp, O. K. Farha, C. J. Cramer and K. W. Chapman, *J. Am. Chem. Soc.*, 2016, **138**, 4178–4185.
29 X. H. Xiong, L. Song, W. Wang, H. T. Zheng, L. Zhang, L. L. Meng, C. X. Chen, J. J. Jiang, Z. W. Wei and C. Y. Su, *Adv. Sci.*, 2024, **11**, 2308123.
30 A. Demessence, D. M. D'Alessandro, M. L. Foo and J. R. Long, *J. Am. Chem. Soc.*, 2009, **131**, 8784–8786.
31 Q. Min Wang, D. Shen, M. Bülow, M. Ling Lau, S. Deng, F. R. Fitch, N. O. Lemcoff and J. Semanscin, *Microporous Mesoporous Mater.*, 2002, **55**, 217–230.
32 J. A. Mason, K. Sumida, Z. R. Herm, R. Krishna and J. R. Long, *Energy Environ. Sci.*, 2011, **4**, 3030–3040.
33 O. Shekhah, Y. Belmabkhout, Z. Chen, V. Guillerm, A. Cairns, K. Adil and M. Eddaoudi, *Nat. Commun.*, 2014, **5**, 4228.
34 X. Si, C. Jiao, F. Li, J. Zhang, S. Wang, S. Liu, Z. Li, L. Sun, F. Xu, Z. Gabelica and C. Schick, *Energy Environ. Sci.*, 2011, **4**, 4522–4527.
35 Y. Lin, C. Kong and L. Chen, *RSC Adv.*, 2012, **2**, 6417–6419.
36 P. Q. Liao, X. W. Chen, S. Y. Liu, X. Y. Li, Y. T. Xu, M. Tang, Z. Rui, H. Ji, J. P. Zhang and X. M. Chen, *Chem. Sci.*, 2016, **7**, 6528–6533.
37 C. P. Cabello, G. Berlier, G. Magnacca, P. Rumori and G. T. Palomino, *CrystEngComm*, 2015, **17**, 430–437.
38 G. Chang, Z. Shang, T. Yu and L. Yang, *J. Mater. Chem. A*, 2016, **4**, 2517–2523.

